Fluorescent Nitric Oxide Photodonors Based on BODIPY and Rhodamine Antennae

Fluorescent Nitric Oxide Photodonors Based on BODIPY and Rhodamine Antennae

Cristina Parisi,[a]† Mariacristina Failla,[a,b] † Aurore Fraix[a] Barbara Rolando,[b] Eleonora Giaquinto,[b] Francesca Spyrakis,[b] Elena Gazzano,[c] Chiara Riganti,[c] Loretta Lazzarato,*[b] Roberta Fruttero,[b] Alberto Gasco[b] and Salvatore Sortino*[a]

Abstract: We report two novel NO photodonors (NOPDs) based on BODIPY and Rhodamine antennae activatable with the highly biocompatible green light. Both the NOPDs exhibit considerable fluorescence emission and release NO with remarkable quantum efficiencies. The combination of the photoreleasing and emissive performance for both compounds is superior to those exhibited by other NOPDs based on similar light-harvesting centres, making them very intriguing for image-guided phototherapeutic applications. Preliminary biological data prove their easy visualization in cell environment due to the intense green and orange-red fluorescence and their photodynamic action on cancer cells due to the NO photo-liberated.

Introduction

Nitric oxide (NO) is a diatomic free radical playing a pleiotropic role in numerous signalling events, including vasodilatation, neurotransmission, inflammation, and immune response in living bodies.[1] Besides, it has proven to be an excellent anticancer, antimicrobial and antioxidant agent.[2] The discovery of such a wealth of properties has profoundly changed the reputation of NO over the last two decades. In fact it has turned to be from a mere environmental pollutant to one of the most studied molecules in the fascinating realm of the biomedical sciences.[1] In this regard, NO offers unique advantages over conventional drugs because it is a multi-target species, does not present Multidrug Resistance issues and, by virtue of its short half-life (< 5 s) and short diffusion radius (< 200 µm) in tissues, confines its reactivity in a restricted region of space. This has stimulated a massive interest in searching and developing of suitable NO donors for research on the bio-function of NO and on its use as “unconventional” therapeutics with exciting prospects in healthcare including cardiovascular, bacterial and cancer diseases.[3] However, the biological effects of NO are closely related to its localization, flux, and transformation.[4] This has made the NO donors activated by light stimuli, namely NO photodonors (NOPDs), very appealing in view of superb spatiotemporal accuracy that can be achieved by tuning the site, duration and intensity of the irradiation source.[5] For a more appropriate therapeutic use of NOPDs, their visualization in a cellular environment remain highly desirable. Fluorescence represents a powerful tool to fulfil this need in a non-invasive way through the aid of fluorogenic components, offering great prospects for image-guided phototherapies based on NO.[6] In fact, excitation of the NOPD with low intensity light generates fluorescence emission, which allows its tracking in cells. Afterwards, excitation with high intensity light can provide a highly localized “burst” of NO precisely at the desired sites.

On the basis of the above considerations the development of new fluorescent NOPDs activable with the biocompatible Vis light, and preferably involving simple synthetic procedures, represents a challenging objective to pursue for widespread use in biologically-oriented labs. In this regard, organic NOPDs do not present toxicity issues related to the transition metals that, in general, may potentially represent a drawback in the case of metal complexes-based NO generators, although these latter offer superior photochemical performances.[5c-e]

Only very recently, limited examples of organic NOPDs activable with one-photon Vis light have been reported.[7] In this scenario BODIPY and Rhodamine derivatives are suitable chromogenic scaffolds to achieve NOPDs working under excitation with the more biocompatible green-orange light, by virtue of their intense absorption and emission properties in this spectral range. However, despite some BODIPY-based NOPDs exhibited good fluorescence emission, the NO photorelease quantum yield (Φ_{NO}) was on the order of 10^{-3} and the quantum efficiency ($\varepsilon_{max}\Phi_{NO}$) did not exceed 550.[7b-d] On the other hand, in the case of Rhodamine-based NOPDs the typical fluorescence emission of this fluorogenic unit is dramatically quenched before the NO photorelease takes place.[7f-h]

In this paper we have designed and synthetized the two novel NOPDs **1** and **2** (Scheme 1) based on BODIPY and Rhodamine light harvesting antennae, which combine clean NO release, exclusively photoregulated by the highly biocompatible single photon green light, and good fluorescence emission performances in the green and orange-red region, respectively

[a] Dr. C. Parisi, Dr. M. Failla, Dr. A. Fraix, Prof. S. Sortino
Laboratory of Photochemistry, Department of Drug Sciences
University of Catania, I-95125 Catania, Italy
E-mail: ssortino@unict.it

[b] Dr. B. Rolando, Dr. E. Giaquinto, Prof. F. Spyrakis, Prof. L. Lazzarato, Prof. R. Fruttero, Prof. A. Gasco
Department of Science and Drug Technology
University of Torino. Via Pietro Giuria 9, 10125 Torino (Italy)
E-mail: loretta.lazzarato@unito.it

[c] Dr. E. Gazzano, Prof. C. Riganti,
Department of Oncology, University of Torino, Via Santena 5/bis, 10126 Torino (Italy)

† Contributed equally

Supporting information for this article is given via a link at the end of the document.

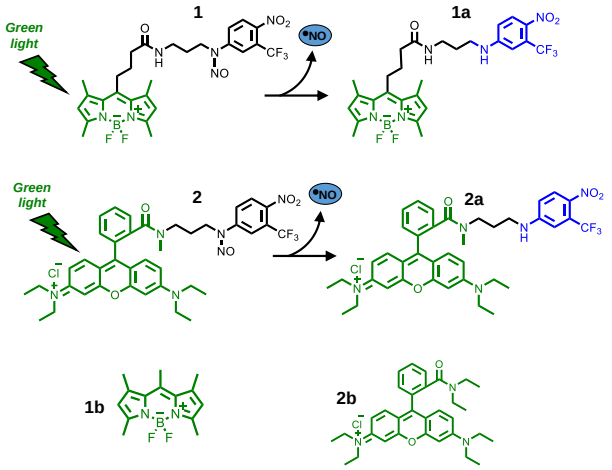

Scheme 1. Structures of the NOPDs **1** and **2**, their main stable photoproducts **1a** and **2a** and the model compounds **1b** and **2b**.

Results and Discussion

Compounds **1** and **2**, synthesized according to the procedures shown in Scheme S1 and S2, were devised in such a way to stimulate the NO release from a N-nitrosoaniline appendage upon excitation of the antennae units.Photoexcitation of the NOPDs **1** and **2** results in the intense green and orange-red fluorescence emissions, typical of the BODIPY and Rhodamine fluorogenic cores (Figure 1). The fluorescence quantum yields, Φ_f, were 0.20 and 0.22 for **1** and **2**, respectively, and the related fluorescence decays exhibited in both cases a dominant component of 1.80 ns and 1.43 ns (insets Figure 1).

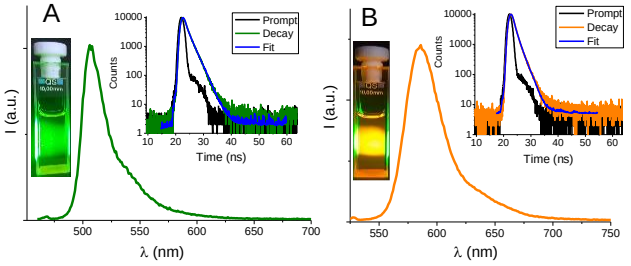

Figure 1. Fluorescence emission spectra and actual images of solutions of **1**, λ_{exc} = 470 nm, (A) and **2**, λ_{exc} = 510 nm, (B). The insets show the fluorescence decay and the related fitting of the same solutions recorded at λ_{exc} = 455 nm and λ_{em} = 504 nm (A) and λ_{exc} = 455 nm and λ_{em} = 582 nm (B). H_2O: MeOH (20:80 v/v). T = 25 °C

The relevant values of Φ_f allowed the clear observation of the fluorescent emission, even at naked eye (see insets Figure 1). Note that, the Φ_f obtained are smaller than those observed in the same solvent for the model compounds **1b** and **2b** (0.90 and 0.30, respectively), which do not present the *N*-nitrosoaniline appendages. Accordingly, the observed fluorescence decays of **1** and **2** were faster than those of **1b** and **2b**, which exhibited dominant components of 5.60 ns and 1.84 ns (Figure S1). These results suggest that a photoprocess competitive with the fluorescence emission occurs in both **1** and **2** (*vide infra*).

Irradiation of solutions of **1** and **2** with green light, leads to the absorption spectral changes illustrated in Figure 2. In both cases, they show the formation of a new absorption at *ca.* 380 nm and the presence of clear isosbestic points, which are indicative of the occurrence of very clean photochemical reactions. Interestingly, the spectra observed at the end of the photolysis are almost identical to those of the non-nitrosated compounds **1a** and **2a** (Figures S2), characterized by the band at 380 nm arising from of the push-pull character of the nitroaniline moiety. HPLC analysis carried out with the autentical compounds **1a** and **2a** as references, confirmed they to be the main stable photoproducts (Figure S3,S4).

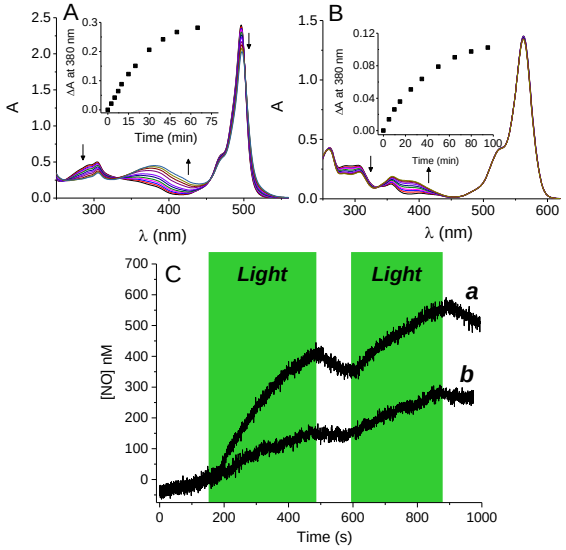

Figure 2. Absorption spectral changes observed upon exposure of a solution of (A) **1** (28 μM) at λ_{exc} = 515-520 nm for intervals from 0 to 65 min and (B) **2** (13 μM) at λ_{exc} = 532 nm for intervals from 0 to 95 min. The arrows indicate the course of the spectral profile with the illumination time. The insets show the difference absorbance changes at λ = 380 nm. H_2O: MeOH (20:80 v/v). T = 25 °C. (C) NO release profiles observed upon green light irradiation of a solution of (*a*) **1** (4.5 μM) (λ_{exc} = 510 nm) and (*b*) **2** (30 μM) (λ_{exc} = 532 nm). H_2O:MeOH (20:80 v/v). T = 25 °C.

Interestingly, the photolysis profiles were identical in the case of N_2-saturated solutions (data not shown), suggesting that the presence of oxygen affects neither the nature nor the efficiency of the photochemical reactions. These findings rule out the participation of the long-lived excited triplet states of **1** and **2** in the photodecomposition processes, according to the well-known inefficiency of population of triplets for BODIPY and Rhodamine derivatives which do not contains heavy atoms in their molecular structures.[8]

Formation of **1a** and **2a** clearly suggests the photorelease of NO from **1** and **2** upon green light excitation. This was demonstrated by the direct detection of NO through amperometric techniques using an ultrasensitive NO

electrode. Figure 2C shows that NO release by both NOPDs takes place exclusively under light stimuli whereas stops in the dark and restarts again once the light is turned on. The quantum yield for the NO photorelease of **1** and **2**, Φ_{NO}, were 0.031±0.001 and 0.001±0.0002, respectively. Note that, the value observed for **1** is more than one order of magnitude larger than that observed for other organic NOPDs based on BODIPY derivatives.[7b-d] Furthermore, the quantum efficiency, expressed as the product of $\varepsilon_{max}\Phi_{NO}$, is *ca.* 2800, a value well superior to those reported for other organic NOPDs.[7a-d] In the case of **2**, the value observed for Φ_{NO} is similar to other Rhodamine derivatives that, however, exhibit fluorescence quantum yields more than one order of magnitude lower than compound **2**.[7f-h]

Since the BODIPY and Rhodamine units are the sole antennae absorbing the green light, photorelease of NO from the nitro-derivative moiety must necessarily involve an electronic communication between these two components. Photoinduced energy transfer from the excited antennae to the nitroso-derivative appendage is, of course, out of question because it is thermodynamically uphill.[9] More likely, the uncaging of NO from **1** seems to be triggered by a photoinduced electron transfer from the *N*-nitrosoaniline-derivative moiety, as electron donor, to the excited singlet states of the antennae, as electron acceptors, according to what recently observed by Nakagawa *et al.*[7d] and by our group[7c] for other BODIPYs linked to nitrosoderivative moieties. In our case, as illustrated in Scheme 2, this process may strongly encourages the detachment of NO from **1** and **2**, due to the generation of an anilino radical derivative after a back electron transfer. This species is very stable due to the presence of the electron drawing nitro and trifluoromethyl groups, is expected to be basically insensitive to the presence of oxygen and that can evolve to the stable photoproducts **1a** and **1b** *via* H-transfer from solvent. This picture is in excellent agreement with the identical photolytic behavior we observed in aerobic and anaerobic conditions and accords well to what already reported the photoproducts formed by other *N*-nitrosamine after loss of NO.[7g,h] Furthermore, our proposal is supported by the considerable changes in free energy for the photoinduced electron transfer processes, $\Delta G \cong -0.5$ eV and –0.3 eV for compound **1** and **2**, estimated by the Rehm-Weller equation:[10]

$$\Delta G = e[E_{ox} - E_{red}] - E_{0,0}$$

where E_{ox} is the half-wave potential for one-electron oxidation of the electron-donor unit, *ca.* 1 eV *vs.* SCE,[11] E_{red} is the half-wave potential for one-electron reduction of the electron-acceptor unit, *ca.* –1 eV and *ca.* -0.9 *vs.* SCE for the BODIPY and Rhodamine antenna, respectively,[12,13] and $E_{0,0}$ is the energy of the lowest excited singlet states of the light harvesting centers, *ca.* 2.5 eV and 2.2 eV for the BODIPY and Rhodamine antennae, respectively.[14] The emissive properties displayed by **1** and **2** if compared with the related model compounds **1b** and **2b** (lower Φ_f values and faster emission decays of the former with respect to the latter) are in excellent agreement with photoinduced processes occurring in the excited singlet states competitive with the fluorescence emission (*vide supra*).

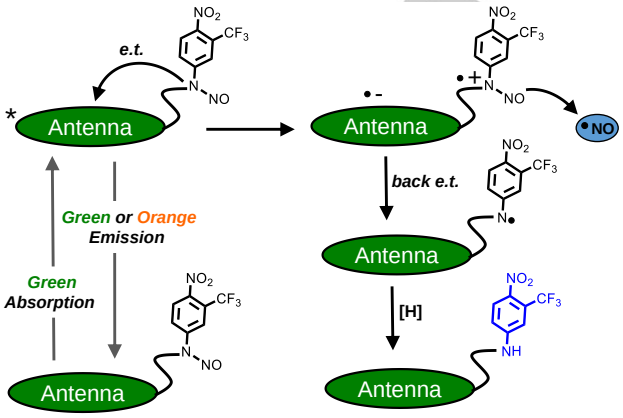

Scheme 2. Proposed mechanism for the NO release triggered by green light from the NOPDs **1** and **2**.

Such photoinduced electron transfer between two species separated by insulator spacers like in the case of **1** and **2** requires, of course, their very close spatial proximity. The flexible spacers present in both compounds strongly encourages this condition. To further verify this hypothesis, we submitted compound **1** and **2** to Molecular Dynamics (MD) simulations. In the two 20 ns-long replicas compound **1** assumes a U-shape conformation for most of the time (Figure 3A). The nitrosoaniline moiety easily folds on the BODIPY, likely forming hydrophobic or π-π interactions. All rings, A, B and C, of BODIPY are alternatively involved, even if A and C more easily pair with the nitrosoaniline. The distance between the nitrogen bearing the NO in the para-nitro-N-nitrosoaniline and the centroid of the A and C rings, tracked along the entire trajectory, is reported in Figure S5. In the first replica the pairing involves mainly ring C, while in the second replica, ring A is more easily paired with the nitrosoaniline. The lower average distance between the nitrogen and the BODIPY have been estimated equal to 5,89 Å and 6,52 Å in replica 1 and 2, respectively.

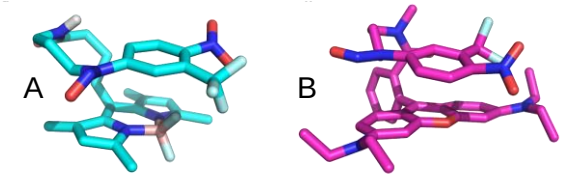

Figure 3. Collapsed U-shaped conformation assumed by compounds **1** (A) and **2** (B) during the MD simulations.

Similarly, in compound **2** the nitrosoaniline folds on the xanthene cycle, making hydrophobic or π-π interactions (Figure 3B). As well, the distance between the nitrogen bearing the NO and the centroid of the A and C rings has been measured in both replicas and reported in Figure S6. In this case, possibly because of the smaller hindrance of the

xanthene cycle with respect to BODIPY, the compound always maintains a collapsed conformation. The lower average distance between the nitrogen and the xanthene have been estimated equal to 4,63 Å and 4,42 Å in replica 1 and 2, respectively.

The remarkable fluorescence of both compounds permits their intracellular localisation by fluorescence microscopy. Figure 4 shows the intracellular localization of **1** or **2** in melanoma cells treated with either **1** or **2**. The typical green fluorescence of **1** and red fluorescence of **2** were well detected intracellularly: the localization of **1** was both mitochondrial and cytosolic, while **2** was mainly accumulated within mitochondria.

Preliminary cytoxicity tests against A375 and SKMEL28 melanoma cancer cells were also performed in the dark and upon green light irradiation (Figure S7). We observed that **1** does not elicit significant cytotoxicity in the dark up to concentration of 10 µM, concentration at which, on the other hand, it induces toxicity only upon irradiation. Compound **2** has higher intrinsic cytotoxicity and was therefore used at lower concentrations, to perform the assays – in the dark – with a reduction in cell viability no > 20%. 2.5 µM was the concentration that reduced cell viability in a not significant way (i.e. to 80% viable cells) compared to the untreated cells. The same concentration however displayed significant cytotoxicity under light.

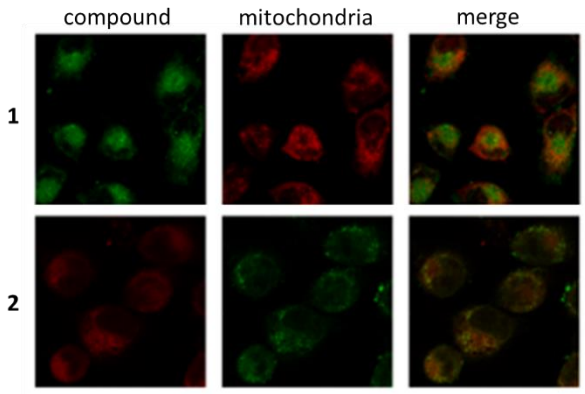

Figure 1. Confocal microscopy analysis of A375 cells. Cells were incubated 4 h with 5 µM **1** or **2**. Cells were then stained with anti-porin/VDAC antibody, followed by TRITC- or FITC-conjugated secondary antibody, to label mitochondria. The image is representative of 1 out of 3 experiments.

Conclusions

In summary, we have reported two novel fluorescent NOPDs, prepared through simple synthetic steps, whose clean NO release is exclusively controlled by the highly biocompatible green light. Both compounds display combinations of the NO photoreleasing and emissive performances superior to those exhibited by other NOPDs based on similar light-harvesting centres. In fact, the BODIPY derivative **1** shows fluorescence efficiency similar to other BODIPY-based NOPDs but NO photorelease efficiency about one order of magnitude larger. On the other hand, the Rhodamine derivative **2** exhibits NO photorelease efficiency similar to other Rhodamine-based NOPDs but fluorescence yield more than one order of magnitude larger. The easy localization in different cell environments of both NOPDs due to their intense green and orange-red fluorescence and their photodynamic activity on cancer cells due to the NO photoreleased make these NOPDs suitable for a widespread use in biologically-oriented labs for research fields where spatiotemporal controlled delivery of NO is required and may open up intriguing prospects for image-guided phototherapeutic applications.

Experimental Section

Chemicals

All chemicals were purchased by Sigma-Aldrich and used as received. Organic solvents were removed under reduced pressure at 30 °C. Synthetic-purity solvents were used. All solvents used for the spectrophotometric studies were spectrophotometric grade. The plastic ware for cell cultures was obtained from Falcon (Becton Dickinson, Franklin Lakes, NJ).

Instrumentation

^{1}H and ^{13}C NMR spectra were recorded on a Jeol ECZ-R 600, at 600 and 150 MHz, respectively, using $SiMe_4$ as internal standard. The following abbreviations are used to designate peak multiplicity: s = singlet, d = doublet, t = triplet, m = multiplet, bs = broad singlet. ESI-MS spectra were recorded on a Micromass Quattro API micro (Waters Corporation, Milford, MA, USA) mass spectrometer. Data were processed using a MassLynx System (Waters). Purity of final compounds (+95%) was determined by analytical HPLC analyses. The reverse-phase HPLC analyses that allowed separation and quantitation of compound **1**, **1a**, **2**, and **2a** were performed with a HP 1100 chromatograph system (Agilent Technologies, Palo Alto, CA, USA) equipped with a quaternary pump (model G1311A), a membrane degasser (G1379A), a diode-array detector (DAD) (model G1315B) integrated in the HP1100 system. Data analysis was done using a HP ChemStation system (Agilent Technologies). The analytical column was a LiChrospher RP-18e 100 A (250 × 4.6 mm, 5 µm particle size) (Merck, Darmstadt, Germany). The mobile phase consisting of acetonitrile/water (80/20 v/v) with 0.1% trifluoroacetic acid and the flow-rate was 1 mL/min. The injection volume was 20 µL (Rheodyne, Cotati, CA). The column effluent was monitored at 480 or 564 nm referenced against 800 nm wavelength. Quantitation was done by comparison of peak areas with standards chromatographed under the same conditions.UV-Vis spectra absorption and fluorescence emission spectra were recorded with a JascoV-560 spectrophotometer and a Spex Fluorolog-2 (mod. F-111) spectrofluorimeter, respectively, in air-equilibrated solutions, using either quartz cells with a path length of 1 cm. Fluorescence lifetimes were recorded with the same fluorimeter equipped with a TCSPC Triple Illuminator. The samples were irradiated by a pulsed diode excitation source Nanoled at 455 nm. The kinetic was monitored at 504 and 582 nm and each solution itself was used to register the prompt at 455 nm. The system allowed measurement of fluorescence lifetimes from 200 ps. The multiexponential fit of the fluorescence decay was obtained using the following equation:

$$I(t) = \Sigma\alpha_i \exp(^{-t/\tau i})$$

Photolysis experiments were performed by irradiating the samples in solution in a thermostated quartz cell (1 cm pathlength, 3 mL capacity)

under gentle stirring, by using a 90 W LED (λ_{exc} = 515-520) and a 30 mW continuum laser (λ_{exc} = 532 nm) having a beam diameter of ca. 1.5 mm. Direct monitoring of NO release for samples in solution was performed by amperometric detection with a World Precision Instrument, ISO-NO meter, equipped with a data acquisition system, and based on direct amperometric detection of NO with short response time (< 5 s) and sensitivity range 1 nM – 20 µM. The analog signal was digitalized with a four-channel recording system and transferred to a PC. The sensor was accurately calibrated by mixing standard solutions of $NaNO_2$ with 0.1 M H_2SO_4 and 0.1 M KI according to the reaction:

$$4H^+ + 2I^- + 2NO_2^- \rightarrow 2H_2O + 2NO + I_2$$

Irradiation was performed in a thermostated quartz cell (1 cm pathlength, 3 mL capacity) using the above continuum laser with λ_{exc} = 532 nm or the 510 nm excitation light of the Fluorolog fluorimeter described above. NO measurements were carried out under stirring with the electrode positioned outside the light path in order to avoid NO signal artefacts due to photoelectric interference on the ISO-NO electrode.

Fluorescence and photodecomposition quantum yields.

Fluorescence quantum yields (Φ_f) were determined using optically-matched solutions at the excitation wavelength of compounds **1** and **1b**, and **2** and **2b**. Solutions of compound **1b** in methanol (Φ_f = 0.95)[15] and Rhodamine B in EtOH (Φ_f = 0.79)[16] were used standards and Φ_f were calculated through the following equation:

$$\Phi_f = \Phi_{f\,(s)}\,(In^2/I_{(s)}n^2_{(s)})$$

where $\Phi_{f\,(s)}$ is the fluorescence quantum yield of the standard; I and $I_{(s)}$ are the areas of the fluorescence spectra of compounds and standard, respectively; n and $n_{(s)}$ are the refraction index of the solvents used for compounds and standard. Absorbance at the excitation wavelength was less than 0.1 in all cases.

Photodecomposition quantum yield was determined at λ_{exc} = 532 nm within the 20% transformation of **1** by using the following equation

$$\Phi_p = [NOPD]xV/t \times x(1–10^{–A})xI$$

where [NOPD] is the concentration of phototransformed NOPD, V is the volume of the irradiated sample, t is the irradiation time, A is the absorbance of the sample at the excitation wavelength and I the intensity of the excitation light source. The concentration of the phototransformed **1** was determined both spectrophotometrically, by taking into account the absorption changes at 380 nm and a $\Delta\varepsilon_{380}$ = 7100 M^{-1} cm^{-1}, and by HPLC analysis. I was calculated by potassium ferrioxalate actinometry.

Computational details

Compounds **1** and **2** were parametrized with the GROMOS G54A7 all-atoms force field.[17] Molecular orbitals were calculated using the Self-Consistent Field (SCF) semi-empirical method and charges were calculated by the Molecular Orbital PACkage (MOPAC).[18] The Automated Topology Builder (ATB) and Repository version 3.0, was used MD setup, simulations and analyses were performed with GROMACS 4.6.1.8S Ligands were explicitly solvated in a cubic box of SPC/E water molecules, charges were neutralized with sodium chlorine, when necessary. Periodic boundary conditions were set, the Particle Mesh Ewald (PME) method was applied for modelling long-range electrostatic interactions that were cut off at 11 Å, the LINCS algorithm was employed for constraining all hydrogen-carbon bonds. Pressure was controlled by coupling the system to a Parrinello-Rahman barostat, temperature was regulated by rescaling velocities. The solvated ligands were minimized by 5000 cycles of steepest descendant algorithm. Three subsequent equilibration steps in the NVT ensemble were performed to progressively heat the systems from 0 to 100 K, from 100 to 200 K, and from 200 to 300 K, respectively. Then, equilibrium pressure condition was accomplished after a final 1ns-long equilibration at 300 K in the isochoric/isobaric (NPT) ensemble. MD trajectories were sampled at 300 K in the NVT ensemble for 20 ns. For each ligand two replicas were run upon velocity rescaling.

Biological assays

Cells. Human melanoma A375 or SKMEL28 (ATCC, Manassas, VA) were maintained in DMEM medium supplemented with 10% v/v fetal bovine serum, 1% v/v penicillin-streptomycin, 1% v/v L-glutamine. Cells were maintained in a humidified atmosphere at 37°C, 5% CO2.

Viability assays. Cells were incubated for 4 h with the indicated concentration of 1 or 2, then maintained in the dark or irradiated at room temperature for 30 min with a white LED 90W lamp with an irradiance of 1.75 mW/cm2 and a Bandpass filter 540 nm +/- 40 nm (IFG BP 540-80 HT) . Irradiance was measured with a Delta Ohm HD2302.0 lightmeter equipped with a Delta Ohm LP4771RAD light probe. 48 h (for 1) or 24 h (for 2) after the irradiation, cells were stained with 5% w/v crystal violet aqueous solution in 66% v/v methanol, washed twice with water, solubilized with 10% v/v acetic acid. The absorbance was read at 570 nm, using a Packard EL340 microplate reader (Bio-Tek Instruments, Winooski, VT). The absorbance of untreated cells was considered as 100% viability; the results were expressed as percentage of viable cells versus untreated cells.

Confocal microscope analysis. 0.5 x 105 cells were grown on sterile glass coverslips and incubated with 1 or 2 for 4 h. Cells were rinsed with PBS, fixed with 3.7% w/v paraformaldehyde (diluted in PBS) for 5 min, permeabilized with 0.1% v/v TritonX-100, and incubated for 1 h at room temperature with an anti-porin/VDAC antibody (1:100, Abcam, Cambridge, UK), followed by the fluorescein isothiocyanate (FITC) or tetramethyl rhodamine isothicyanate (TRITC)-secondary antibody (1:50, Abcam), to label mitochondria. Cells were washed three times with PBS then the slides were mounted with 10 µl of Gel Mount Aqueous Mounting (Sigma). The samples were analyzed with an Olympus FV300 laser scanning confocal microscope equipped with a Blue Argon (488 nm) laser, a Green Helium Neon (543 nm) laser, and FluoView 300 software (Olympus Biosystems, Hamburg, Germany). For each experimental conditions, 5 fields were examined.

Statistical analysis. Data are provided as means+SD. The results were analyzed by a one-way ANOVA and Tukey's test. $p < 0.05$ was considered significant.

Acknowledgements

We thank AIRC Project IG-19859 and Ricerca Locale from the University of Turin for financial support.

Keywords: Light • Fluorescence • Nitric oxide • Photochemistry

[1] *Nitric Oxide: Biology and Pathobiology*, ed. Ignarro, L. J. Elsevier Inc., **2010**; Special Journal Issue on *Nitric Oxide Chemistry and Biology*. Ed. Ignarro, L. J. *Arch. Pharmacal Res*. 2009.

[2] a) D. Fukumura,S. Kashiwagi, R. K. Jain, *Nat. Rev. Cancer,* **2006,** *6*, 521-534; b) F. C. Fang, *J. Clin. Invest*., **1997**, *99*, 2818-2825; c) Methods in Enzymology, Vol. 301: Nitric Oxide, Part C: Biological and Antioxidant Activities, Ed. Packer, Lester; Academic, San Diego, **1999**.

[3] a) A. W.Carpenter, M.- H. Schoenfisch, *Chem. Soc. Rev.,* **2012**, *41*, 3742-3752; b) P. G. Wang, M. Xian, X. Tang, X. Wu, Z. Wen, T. Cai, A. J. Janczuk, *Chem. Rev.* **2002**, *102*, 1091-1134. c) Nitric oxide donors; P. G. Wang, T. B. Cai, N. Taniguchi, Eds., Wiley-VCH: Weinheim, **2005**.

[4] a) Z. Huang, J. Fu, Y. Zhang, *J. Med. Chem.,* **2017**, *60*, 7617–7635.

[5] a) S. Sortino, *Chem. Soc. Rev.,* **2010**, *39***,** 2903-2913; b) A. Fraix, S. Sortino, *Photochem. Photobiol Sci*. **2018**, *17*, 1709–1727; c) P. C. Ford, *Acc. Chem. Res*., **2008**, *41*, 190-200; d) P. C. Ford, *Nitric Oxide,* **2013**, *34*, 56-65; e) N. L. Fry, P. K. Mascharak, *Acc. Chem. Res*., **2011**, *44*, 289-298;

[6] A. Fraix, S. Sortino, *Chem. Asian J.,* **2015**, *10*, 1116-1125.

[7] a) E. B. Caruso, S. Petralia, S. Conoci, S. Giuffrida, S. Sortino, *J. Am. Chem. Soc*., **2007**, *129*, 480-481; *b)* M. Blangetti, A. Fraix, L. Lazzarato, E. Marini, B. Rolando, F. Sodano, R. Fruttero, A. Gasco, S. Sortino, *Chem. Eur. J.*, **2017**, *23*, 9026-9029; c) C. Parisi, M. Failla, A. Fraix, A. Rescifina, B. Rolando, L. Lazzarato, V. Cardile, A. C. E. Graziano, R. Fruttero, A. Gasco, S. Sortino, S. *Bioorg. Chem.* **2019***, 85, 18–22;* d) N. Ieda, Y. Hotta, N. Miyata, K. Kimura, H. Nakagawa, *J. Am. Chem. Soc*., **2014**, *136*, 7085-7091; e) E. Y. Zhou, H. Knox, C. J. Reinhardt, G. Partipilo, M. J. Nilges, J. Chan, *J. Am. Chem. Soc*. **2018**, *140*, 11686–11697; f) K. Kitamura, M. Kawaguchi, N. Ieda, N. Miyata H. Nakagawa, *ACS Chem. Biol.*, **2016**, *11*, 1271-1278*;* g) H. He, Y. Xia, Y. Qi, H.-Y. Wang, A. Wang, J. Bao, Z. Zhang, F.-G. Wu,H. D. Chen. D. Yang, X. Liang, J. Chen, S. Zhou, X. Liang, X. Qian, Y. Yang, *Bioconjugate Chem.* **2018**, *29*, 1194-1198; h) H. He, Z. Ye, Y. Xiao, W. Yang, Y. Yang, *Anal. Chem.* **2018**, *90*, 2164-2169.

[8] a) J. Zhao, K. Xu, W. Yang, Z. Wang, F. Zhong, *Chem. Soc. Rev.,* **2015**, *44*, 8904—8939; b) P. C. Beaumont, D. G. Johnson, B. J. Parsons, *J. Photochem. Photobiol. A: Chem.,* **1997**, *107, 175-183.*

[9] The excited singlet state of BODIPY and Rhodamine chromophores lie more than 1 eV below that of the nitroso-derivative unit (estimated by the end of the absorption spectra of these chromophoric units).

[10] D. Rehm, A. Weller, A. *Isr. J. Chem*. **1970**, *8*, 259-262.

[11] E. Lund, *Acta Chem. Scand.* **1957**, *11*, 990-996.

[12] a) K. Krumova, G. Cosa, G. *J. Am. Chem. Soc*., **2010**, *132*, 17560-17569; b) L. Huang, W. Yang, J. Zhao, J. *J. Org. Chem.*, **2014**, *79*, 10240-10255.

[13] M. J. Austin, I. R. Harrison, T. I. Quickenden, *J. Phys. Chem.* **1986**, *90*, 1839-1843.

[14] Estimated by the end of the absorption and the onset of the fluorescence emission spectra of **1** and **2.**

[15] A. Loudet, K. Burgess, *Chem. Rev.*, **2007**, 107, 4891 – 4932.

[16] M. Montalti, A. Credi, L. Prodi, M. T. Gandolfi, Handbook of Photochemistry, 3rd ed., CRC, Boca Raton, **2006**.

[17] N. Schmid, A. P. Eichenberger, A. Choutko, S. Riniker, M. Winger, A. E. Mark, W. F. van Gunsteren *Eur. Biophysics J*., **2011**, *40*, 843-856.

[18] D. Van Der Spoel, E. Lindahl, B. Hess B, et al. *G J Comput Chem* **2005**, *26*, 1701–1718.

Entry for the Table of Contents

ARTICLE

BODIPY and Rhodamine-based NO photodonors activatable by the highly biocompatible green light exhibit superior combination of fluorescence emission and NO release performances making them very intriguing for image-guided phototherapeutic applications.

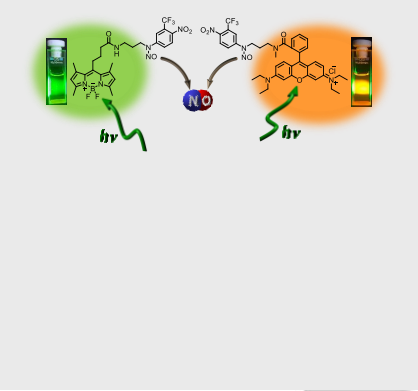

C. Parisi, M. Failla, A. Fraix, B. Rolando, E. Giaquinto, F. Spyrakis, , E. Gazzano, C. Riganti, L. Lazzarato, R. Fruttero, A. Gasco and Salvatore Sortino**

Page No. – Page No.

Fluorescent Nitric Oxide Photodonors Based on BODIPY and Rhodamine Antennae